analytical chemistry

Article

Cite This: *Anal. Chem.* 2019, 91, 3452−3458

pubs.acs.org/ac

Versatile and Ultrasensitive Electrochemiluminescence Biosensor for Biomarker Detection Based on Nonenzymatic Amplification and Aptamer-Triggered Emitter Release

Yamin Nie, Xiaoding Yuan, Pu Zhang, Ya-qin Chai,* and Ruo Yuan*

Key Laboratory of Luminescent and Real-Time Analytical Chemistry (Southwest University), Ministry of Education, College of Chemistry and Chemical Engineering, Southwesongqing 400715, China

Supporting Information

ABSTRACT: Electrochemiluminescence (ECL), as a sensitive and controllable assay, offers a considerable opportunity for multiple types of biomarkers detection. However, constructing such a biosensor remains a significant challenge. Herein, an ultrasensitive and versatile ECL biosensor was constructed to detect multiple types of biomarkers from breast cancer by taking the strategies of nonenzymatic catalytic hairpin assembly (CHA) and hybridization chain reaction (HCR) amplification, as well as aptamer-triggered emitter release. Concretely, with the appearance of target 1 microRNA-21 (miRNA-21), abundant double-stranded DNA (dsDNA) polymers were generated on this biosensing surface via amplification circuits of CHA and HCR, which could be intercalated into substantial ($[Ru(bpy)_2dppz]Cl_2$) as ECL indicators to obtain an obvious enhancement of ECL signal for target 1 detection with a detection limit (0.1 fM). Furthermore, in the presence of target 2 human mucin 1 (MUC1) protein, the ECL signal had a distinct decrease, because aptamer recognition induced the release of $[Ru(bpy)_2dppz]Cl_2$ from the sensing surface, thus, achieving a sensitive detection for MUC1 with a detection limit (2.4 fg·mL^{-1}). Simultaneously, this sensing platform was applied to monitor the biomarkers from MDA-MB-231 breast cancer cells, suggesting that this method was applicable to detect real samples. Therefore, this platform is an applicable and versatile implement for the determination of multiple types of biomarkers to improve diagnostic accuracy and efficiency.

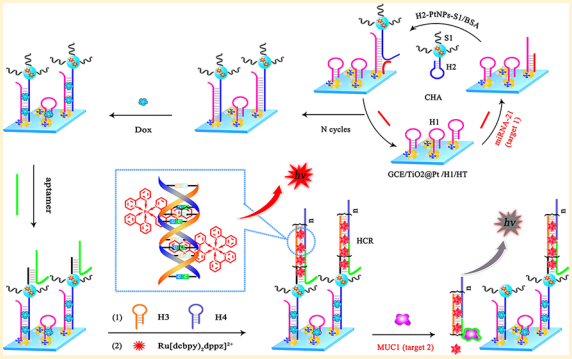

Electrochemiluminescence (ECL) provides a promising application for the determination of cancer biomarkers because of its sensitivity and controllability by ingeniously integrating chemiluminescence with electrochemistry.[1−4] Unfortunately, the existing ECL analysis usually got stuck in monitoring for single biomarker on account of the unavoidable occurrence of cross reactions with diverse emitters in the detection for multiple biomarkers.[5,6] However, monitoring expression levels of cancer-related multiple biomarkers, especially different types of biomarkers, has the ability to reflect more clues, which offers a wide window of opportunity to enhance diagnostic accuracy and efficiency for early diagnosis, possessing significant potential to reduce the harrowing mortality of cancer.[7,8]

To meet the requirement of detection for multiple biomarkers, our group recently has dedicated to take the strategies of controlling the movement of DNA-based nanomachines and employ multivariate linear algebraic equations to maximally avoid cross reactions.[9−11] Nonetheless, these proposed assays are limited to monitoring of the same type of multiple biomarkers with the demand of a sophisticated DNA machine or a complicated mathematical model. Very recently, we designed a platform for the monitoring of both miRNA-141 and MMP-2 proteins by using the method of target-induced cleavage of peptide.[12] Unfortunately, such a platform only adjusted to detect extremely restricted proteins, which could induce the cleavage of peptide.[13,14] Therefore, it is full of challenges and is highly desirable to design a versatile and ultrasensitive system for the determination of microRNA (miRNA) and protein biomarkers for improving diagnostic accuracy and efficiency.

Excitingly, nucleic acid aptamer, single strands of DNA or RNA, could be selected for any given target, in principle, from simple molecule to large protein, and even cells with high binding affinity and specificity, offering an incredibly effective tool in bioanalysis.[15−17] In view of the favorable performance of the nucleic acid aptamer, the determination for various proteins could be achieved with the use of a nucleic acid aptamer as the protein recognition element, which is beneficial to construct a versatile biosensor to monitor multiple types of biomarkers. Moreover, compared with antibody or peptide as a recognition element, aptamer is more favorable to apply DNA amplification technologies to improve the determination sensitivity for proteins.[18−20] Therefore, taking aptamer as

Received: October 31, 2018
Accepted: January 22, 2019
Published: January 22, 2019

DOI: 10.1021/acs.analchem.8b05001
Anal. Chem. 2019, 91, 3452−3458

Scheme 1. Schematic Illustration of the Versatile and Ultrasensitive Electrochemiluminescence Biosensor for the Monitoring of miRNA-21 and MUC1 from Breast Cancer

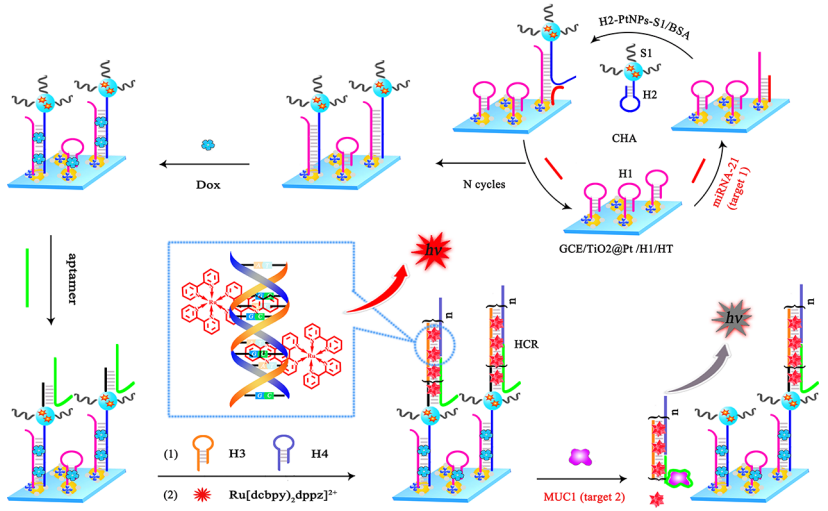

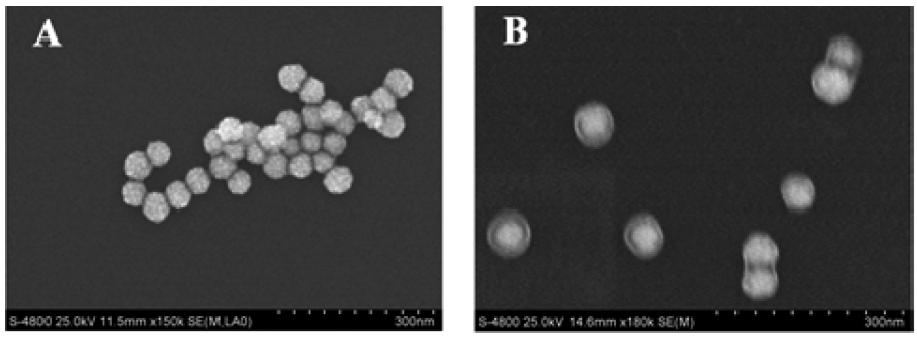

Figure 1. SEM characterization of (A) PtNPs and (B) H2-PtNPs-S1.

protein recognition element and integrating DNA amplification technique are beneficial to construct a versatile and ultrasensitive biosensor to detect miRNA and protein biomarkers.

Herein, a versatile and ultrasensitive ECL sensing platform was developed to detect microRNA-21 (miRNA-21) and MUC1 protein with single ECL indicator for overcoming the unavoidable cross reactions. As depicted in Scheme 1, H1 was first incubated on the TiO_2@Pt modified sensing surface via a Pt−S covalent bond. Then, target 1 miRNA-21, the catalyst of catalytic hairpin assembly (CHA) reaction, hybridized with H1 to form H1/miRNA-21 intermediate that further initiated the dynamic assembly of H2 on the H2-PtNPs-S1 bioconjugates and simultaneously released miRNA-21 to trigger another cycle, leading to immobilization of the abundant bioconjugates on the sensing surface. After that, doxorubicin (Dox) was incubated on the biosensor to intercalate into double-stranded DNA (dsDNA) for avoiding false positive signal. Afterward, aptamer was introduced to hybridize with S1 on the surface of H2-PtNPs-S1 bioconjugates and activates hybridization chain reaction (HCR) amplification with H3 and H4, generating numerous double-stranded DNA (dsDNA) polymers. Subsequently, $[Ru(bpy)_2dppz]^{2+}Cl_2$, a novel "light-switch" molecule as ECL emitter, was embed in the formed dsDNA polymers to provoke a significant enhance of ECL intensity for the ultrasensitive analysis of target 1 with a detection limit (0.1 fM). In the presence of target 2 MUC1 protein, the $[Ru(bpy)_2dppz]^{2+}Cl_2$ released from biosensing surface owing to the strong affinity of MUC1 with its aptamer, leading to a sharply decrease of ECL intensity to realize the determination for MUC1 protein with a detection limit (2.4 $fg{\cdot}mL^{-1}$). Significantly, the sensing platform successfully monitored multiple types of biomarkers extracting from MDA-MB-231 breast cancer cells with high sensitivity, highlighting that this versatile and ultrasensitive platform has promising potential to improve diagnostic accuracy and efficiency for cancer.

EXPERIMENTAL SECTION

The descriptions of "Materials and Reagents", "Apparatus and Measurements", "Preparation and Characterization of TiO_2@Pt", and "Cell Culture and the Extraction" are described in the Supporting Information.

Assembly Process for This Sensing Platform. The step-by-step fabrication of the biosensing platform was illustrated in Scheme 1. The glassy carbon electrode (GCE, Φ = 4 mm) was first prepared referring to literature.[12] Afterward, 10 μL of TiO2@Pt solution (the preparation and characterization of TiO2@Pt nanoparticles are manifested in the Supporting Information) modified on the prepared electrode and dried. A total of 10 μL of H1 solution (2 μM) was incubated overnight on the biosensor surface and then immersed with HT (1 mM) for 40 min for blocking nonspecific binding sites. Next, a total of solution with a 5 μL series of concentrations of target 1 (miRNA-21) and 5 μL of H2-PtNPs-S1 bioconjugates were incubated for 2 h at 37 °C to trigger CHA amplification. After that, 10 μL of Doxorubicin (Dox, 2 mM) was incubated for 4 h

DOI: 10.1021/acs.analchem.8b05001
Anal. Chem. 2019, 91, 3452−3458

on the sensing surface to intercalate into dsDNA for avoiding unnecessary false positive signal. Following that, 10 μL of aptamer solution (2 μM) was incubated on the above-mentioned surface for 1 h at 37 °C for hybridizing with S1. Then, a mixture of H3 (5 μL, 1 μM) and H4 (5 μL, 1 μM) was incubated on the biosensor to trigger HCR amplification for generating abundant dsDNA polymers. The modified surface further immersed with $Ru(bpy)_2dppz]Cl_2$ solution (5 mM, 10 μL) served as ECL emitter, which could intercalate into dsDNA, achieving a high signal for the sensitive monitoring of target 1 miRNA-21. However, when the relevant sensing electrode incubated with target 2 MUC1 protein, the ECL intensity significantly decreased because the aptamer recognition induced the release of $Ru(bpy)_2dppz]Cl_2$ from the biosensing surface, thus, realizing the sensitive detection of MUC1. Completing each step of the above-mentioned process, the modified electrodes were thoroughly rinsed with deionized water to remove unreacted species and physical adsorption.

RESULTS AND DISCUSSION

Characterization of PtNPs and H2-PtNPs-S1 Bioconjugates. The preparation of the PtNPs was accordance with the procedure described in the literature.[21] The scanning electron microscope (SEM) pictures (Figure 1A) were implemented to validate the morphology feature of the synthetic PtNPs, showing roughly spherical shape with a uniform radius of 44 ± 0.1 nm. However, the surface of nanoparticles becomes blurry with better monodispersity (Figure 1B) after immobilizing H2 and S1 onto the surface of PtNPs through Pt−S bond to form the bioconjugates of H2-PtNPs-S1, because the attachment of H2 and S1 generates an electrostatic layer, providing both electrostatic and steric resistance to reduce aggregation.[22]

Detection Strategy for Multiple Types of Biomarkers. This detection system takes the strategies of CHA and HCR amplification, as well as aptamer recognition-induced the release of ECL indicators to construct a ultrasensitive and versatile ECL biosensor for multiple types of biomarkers detection. To be specific, in the presence of target 1, miRNA-21 successively triggered the CHA and HCR amplification, generating abundant dsDNA polymer. Afterward, $[Ru(bpy)_2dppz]^{2+}Cl_2$, a fashionable "light switch" molecule, which could intercalate into DNA possessing an intense emission but a negligible ECL intensity in aqueous solution[23] (the possible light-emitting mechanism of the $[Ru(bpy)_2dppz]^{2+}$/tri*n*-propylamine (TPrA) system was illustrated in Figure S2), was selected as ECL emitter embedding into formed dsDNA polymer to obtain a significant ECL intensity and detect miRNA-21 (target 1). Then, in the presence of MUC1 protein (target 2), gave rise to the $[Ru(bpy)_2dppz]^{2+}Cl_2$ release from biosensing surface owing to the strong affinity of MUC1 with its aptamer, realizing the detection for MUC1 protein.

Investigation the Feasibility of the Signal Amplification Strategy. Native polyacrylamide gel electrophoresis (PAGE) analysis, as a definitive method, was applied to evaluate the feasibility of the CHA and HCR amplification strategy, and the results were presented in Figure 2. In terms of the investigation of CHA circuit, the control groups (lanes 1, 2, and 4), respectively, corresponded to the bands of H1, H2, and a mixture of H1/H2. As expected, the mixture of H1/H2 displayed original definite bands of monomer of H1 and H2, indicating the CHA amplification was forbidden without target

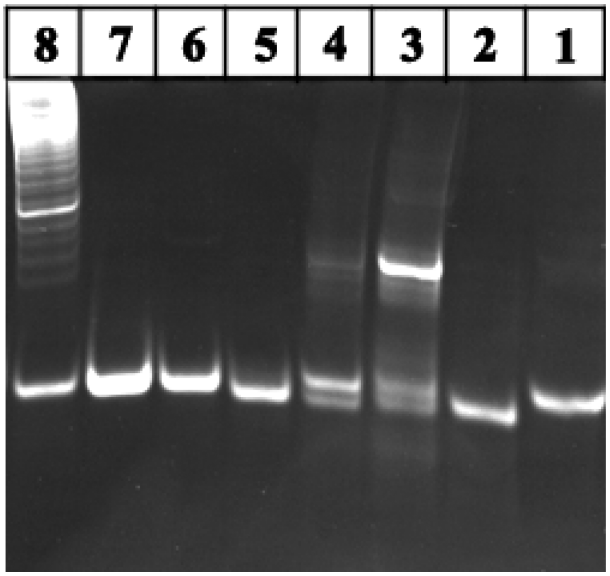

Figure 2. Native PAGE showing the assembly of the amplification strategy: lane 1, H1; lane 2, H2; lane 3, mixture of H1, H2, and miRNA-21; lane 4, mixture of H1 and H2; lane 5, aptamer; lane 6, H3; lane 7, H4; lane 8, mixture of aptamer, H3, and H4.

1 (miRNA-21). However, in the presence of miRNA-21, a lower electrophoretic mobility band could obviously be seen in lane 3, manifesting the successful assembly of the CHA circuit. Meanwhile, we further verified the feasibility of the HCR amplification. The control groups (lanes 5, 6, and 7), respectively, corresponded to the bands of aptamer, H3, and H4. After addition of aptamer with H3 and H4, apparently arose a series of new bright stripes (lane 8) with an obvious low electrophoretic mobility, manifesting that the aptamer could trigger H3 and H4 to generate the amplification of HCR. Therefore, the above results illustrated that the design of the amplification of CHA and HCR was practicable.

EIS Performance of the Developed Biosensor. Electrochemical impedance spectroscopy (EIS), as a powerful technology for interfacial investigation, was introduced to investigate the assembly of this biosensor (Figure 3). After incubation of TiO_2@PtNPs, the semicircle was decrease (curve b) in comparison to the bare GCE (curve a) due to the PtNPs facilitating electron transfer. When successively incubated with negatively charged H1 (curve c) and nonconductive HT (curve d), the semicircle continuously augmented with the increase of electrostatic repulsion and steric hindrance for the redox probe diffusing to the electrode, respectively. Additionally, after the mixtures of target 1 (miRNA-21) and H2-PtNPs-S1 bioconjugates (curve e) were assembled onto the electrode, a decreased resistance generated, which demonstrated the successful CHA process and the fact that the charge transfer promotion of conductive PtNPs surpassed the hindrance of negatively charged DNA strands. Afterward, with the step-by-step fabrication of Dox (curve f), aptamer (curve g), and the mixture of H3 and H4 (curve h), the EIS signal sequentially increased owing to the successful assembly causing the increase of interfacial barrier for the diffusion of ferricyanide. However, when the positively charged ECL probe, $Ru(bpy)_2dppz]^{2+}$, intercalated into dsDNA (curve (i), the resistance dramatically decreased owing to the electrostatic attraction from $[Ru(bpy)_2dppz]^{2+}$ to $[Fe(CN)_6]^{3-/4-}$, facilitating the diffusion for $[Fe(CN)_6]^{3-/4-}$. Nevertheless, in the presence of target 2

DOI: 10.1021/acs.analchem.8b05001
Anal. Chem. 2019, 91, 3452−3458

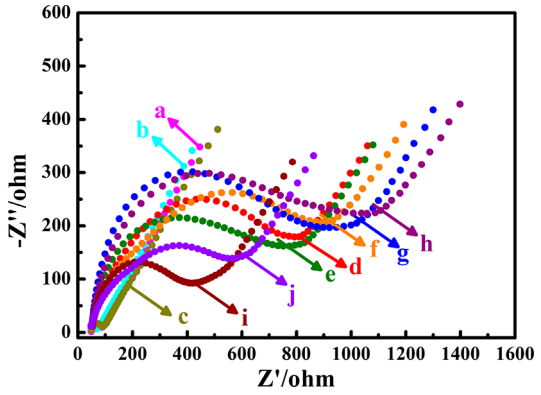

Figure 3. EIS characterization for stepwise fabrication: (a) bare GCE; (b) TiO_2@PtNPs/GCE; (c) step b incubated with H1; (d) step c blocked with HT; (e) step d incubated with the mixture of miRNA-21 and H2-PtNPs-S1 bioconjugates; (f) step e intercalated into Dox; (g) step f hybridized with aptamer; (h) step g triggered HCR amplifier; (i) step h intercalated into $Ru(bpy)_2dppz]^{2+}$; (j) step i incubated with MUC1. The detection was performed in PBS including 5 mM $[Fe(CN)_6]^{3-/4-}$ and 0.1 M KCl.

(MUC1), the EIS response obviously increased owing to the aptamer recognition-induced the release of the dsDNA and $Ru(bpy)_2dppz]^{2+}$. The results indicated the successful construction of this platform.

Analytical Optimization of the Biosensing Platform. Dox, a famous intercalator for double-stranded DNA (dsDNA), was subtly introduced on the sensing surface to embed in the dsDNA containing complementary parts of residual H1 and the forming dsDNA from CHA amplification for avoiding the ECL emitter $Ru(bpy)_2dppz]^{2+}$ to intercalate into the dsDNA causing false positive signal. The effect of Dox was studied with the condition of without miRNA-21. As shown in Figure 4A, with incubation of Dox, the background signal obviously decreased (curve a) compared with the absence of Dox (curve b), suggesting that the Dox could intercalate into dsDNA and thus avoid the false positive signal.

The optimal incubating time of H3 and H4 was explored for improving the sensitivity. Figure 4B displayed the ECL signal augmented in the wake of the increase of incubation time, and there was no distinct change after the incubation time beyond 3 h. Hence, the best incubation time for H3 and H4 was chosen as 3 h.

ECL Performance of the Elaborate Biosensor for the miRNA-21 and MUC1. To evaluate the potential quantitative evaluation of the biosensor for miRNA-21 and MUC1, a series of concentrations of the dual types of biomarkers were monitored. From curve a to curve f (Figure 5A), the ECL intensity sharply augment with the increasing of target 1miRNA-21 (from 1.0 fM to 100 pM). Figure 5B manifested that the increased ECL intensity ΔI revealed a desirable linear correlation with logarithmic value of the miRNA-21 concentration, fitted as ΔI_{ECL} = 43445.19 + 2688.27 lg(c/M) (R^2 = 0.993), where ΔI_{ECL} and c, respectively, represented the increased ECL signal and the miRNA-21 concentration. The estimated limit of detection (LOD) was 0.1 fM[24] (S/N = 3, and the calculation was shown in Supporting Information).

The dependence of ECL response to target 2 (MUC1) was further evaluated when the target 1 concentration served as 100 pM. As displayed in Figure 6A, the ECL intensity intensely reduced with growing concentration of MUC1 (0.01 pg·mL^{-1} to 1000 ng·mL^{-1}). From Figure 6B, the calibration curve showed a pleasurable linear relationship between the decreased ECL intensity (ΔI_{ECL}) and the logarithmic value of MUC1, represented as ΔI_{ECL} = 20095.54 + 1308.91 lg[c/(g·mL^{-1})] (R^2 = 0.996) and a detection limit of 2.4 fg·mL^{-1} (S/N = 3). From above-mentioned results, it can be concluded that this versatile and ultrasensitive platform exhibited a relatively desirable performance compared to that of other multianalyte biosensors (Table S2), exhibiting a promising application for quantitative detection of different types of biomarkers from breast cancer.

Selectivity and Stability for This Biosensing Platform. Diagnostic specificity is a significant issue to evaluate the performance of a biosensor, so the selectivity of this biosensor was investigated. Variable interfering agents containing miRNA-141 (1 nM) and miRNA-155 (1 nM) were, respectively, applied to take the place of the 10 pM of target 1 miRNA-21 to study the selectivity of this biosensor for miRNA-21 since they are always coexisted in breast cancer cells.[25,26] As depicted in Figure 7A, there was a sharply increased ECL signal with the introduction of target miRNA-21 (10 pM) contrast to the blank sample. However, as this sensing platform was incubated with miRNA-141 or miRNA-155, the intensity looked similar to blank sample. In addition,

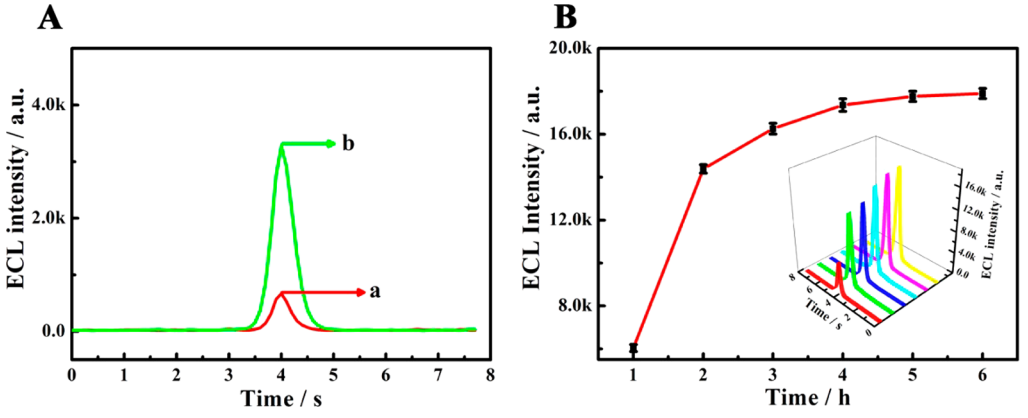

Figure 4. (A) Investigation the effect of Dox for the biosensor: (a) with the incubation of Dox and (b) without the incubation of Dox. (B) Optimum incubation time of H3 and H4 for triggering HCR amplification. The detection was carried out in 0.1 M PBS (pH 7.4), including 20 mM TPrA (scan range: 0 to 1.2 V, vs Ag/AgCl) and a PMT at 800 V.

DOI: 10.1021/acs.analchem.8b05001
Anal. Chem. 2019, 91, 3452−3458

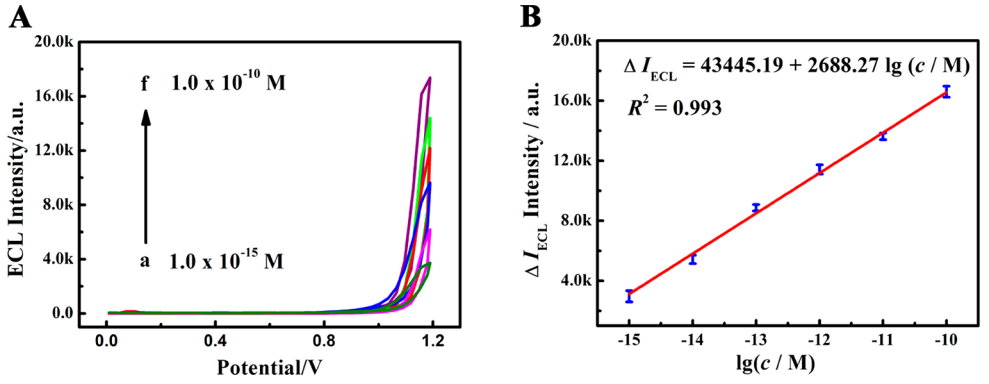

Figure 5. (A) ECL intensity−potential profiles of this biosensor incubating target 1 (miRNA-21) with different concentrations. (B) Calibration plot of ΔI_{ECL} intensity with the logarithm value of miRNA-21 concentration. The experiment was performed in 0.1 M PBS (pH 7.4) including 20 mM TPrA (scan range: 0 to 1.2 V, vs Ag/AgCl) and a PMT at 800 V.

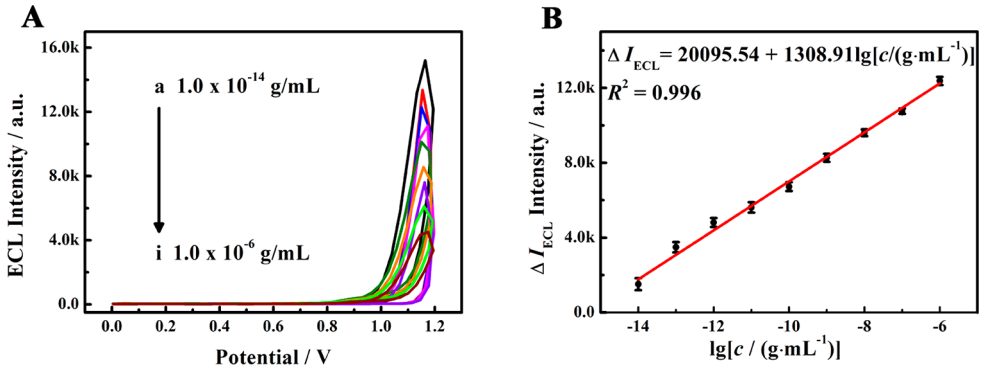

Figure 6. (A) ECL intensity-potential profiles of this platform with variable concentration for target 2 (MUC1). (B) Calibration plot of ΔI_{ECL} intensity vs the logarithm of MUC1 concentration. ECL intensity was detected in 0.1 M PBS (pH 7.4), including 20 mM TPrA (scan range: 0 to 1.2 V, vs Ag/AgCl) and a PMT at 800 V.

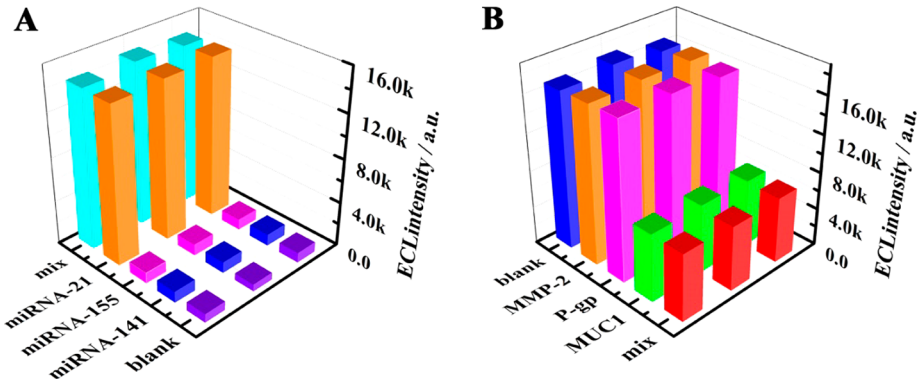

Figure 7. Study of the selectivity performances of the biosensor for multiple types of biomarkers.

the mixture solution containing target miRNA-21 and the above-mentioned interfering substances (each at 10 pM) possessed a nearly negligible change compared with the ECL intensity of only target miRNA-21 (10 pM). Therefore, these results demonstrated this biosensor for miRNA-21 detection presented remarkable specificity.

Subsequently, interfering substances containing 100 ng·mL^{-1} of MMP-2 and 100 ng·mL^{-1} of P-gp, which are coexpressed in breast cancer with a high-level expression,[27,28] were applied to confirm this biosensor selectivity for target 2 MUC1. As illustrated in Figure 7B, there was scarcely any variation in ECL intensity of the interfering substances (MMP-2 or P-gp) than that of the blank sample. However, even at 10-fold lower concentration of target 2 MUC1 (10 ng·mL^{-1}), the ECL response dramatically declined in comparison to the interfering substances. Additionally, for the mixture solution containing MUC1 (10 ng·mL^{-1}) and interfering substances, the ECL intensity was almost the same as the value obtained from MUC1 only. Therefore, such biosensor had excellent specificity for MUC1.

Stability has great significance for assessing the performance for a biosensing system, so the stability for the biosensor was estimated with a continuous cyclic scanning for 10 cycles. As can be seen from Figure 8A, ECL intensity had no visible fluctuation when the sensing biosensor incubated with 10 fM of target 1 miRNA-21 and had a relative standard deviation

DOI: 10.1021/acs.analchem.8b05001
Anal. Chem. 2019, 91, 3452−3458

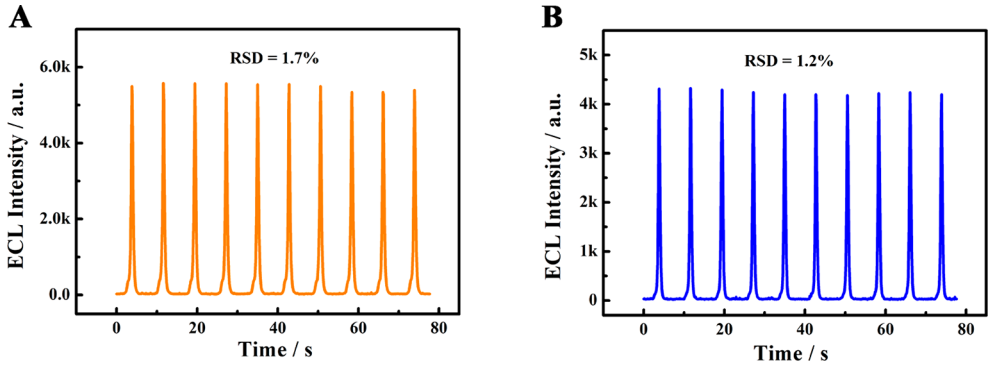

Figure 8. Stability for the developed biosensor.

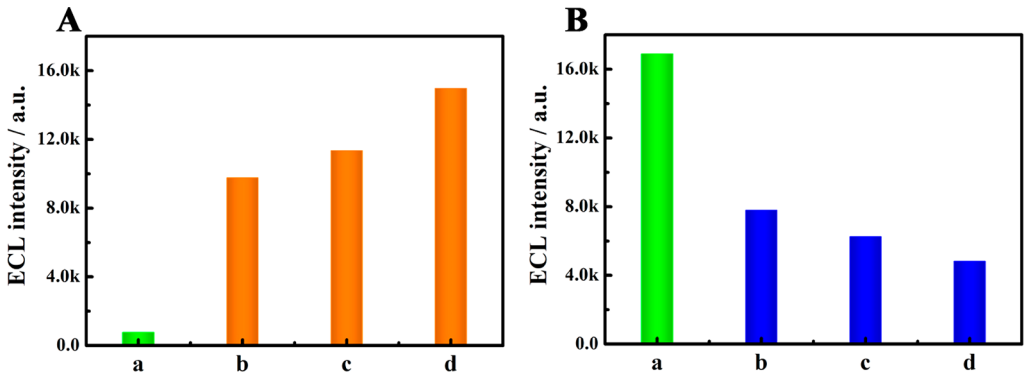

Figure 9. Application of this biosensor to detect different numbers of cancer cells for the analysis of (A) miRNA-21: (a) blank detection, (b) 10^3, (c) 10^4, and (d) 10^5 cells; (B) MUC1: (a) blank detection; (b) 10^4, (c) 10^5, and (d) 10^6 cells.

(RSD) of 1.7%. Furthermore, the ECL signal also had no distinct fluctuation with a RSD of 1.2% after incubating 1000 ng·mL^{-1} target 2 MUC1 protein (Figure 8B). These results indicated that the biosensor possessed a favorable stability. Besides, the biosensor also manifests a pleasurable reproducibility in batch and between batches (Figure S3).

Application of This Biosensor for the Monitoring of miRNA-21 and MUC1 in MDA-MB-231 Breast Cancer Cells. To explore the applicability of this biosensing for practical samples, the lysates of MDA-MB-231 (breast cancer cell lines, both miRNA-21 and MUC1 overexpressed) was conducted with this biosensor. From Figure 9A, the ECL intensity obviously increased with the growing MDA-MB-231 cell numbers (bars b, c, and d) and exhibited apparent differences compared to the blank one (bar a). The obtained results indicated that miRNA-21 overexpressed in MDA-MB-231 cancer cells, showing agreement with previous reports.[29,30] Moreover, as can be figured out in Figure 9B, the ECL intensity had an intense decrease with the increasing cell number (bars b, c, and d) and had an evident distinction with the blank one (bar a), which was in accordance with the reported literature.[31] With this favorable application of this biosensing platform, we offered an ultrasensitive and versatile electrochemiluminescence strategy to monitor multiple types of biomarkers for enhancing cancer diagnostic accuracy and efficiency.

CONCLUSION

In summary, a versatile and ultrasensitive ECL sensing platform was successfully constructed to monitor multiple types of biomarkers with the use of the strategies of enzyme-free signal amplification and aptamer-triggered emitter release, and the system could efficiently avert cross-talk reactions with single ECL luminophore to improve the accuracy of detection. Additionally, the detection studies for miRNA-21 and MUC1 protein from MDA-MB-231 breast cancer demonstrate that this versatile and ultrasensitive platform has great potential to detect multiple types of biomarkers from real samples, which is crucial to improve diagnostic efficiency and accuracy.

ASSOCIATED CONTENT

Supporting Information

The Supporting Information is available free of charge on the ACS Publications website at DOI: 10.1021/acs.analchem.8b05001.

Additional electronic information as pointed in the text. Reagents and apparatus, formation and morphology of TiO_2@Pt, cell culture and the extraction, possible light-emitting mechanism of the $[Ru(bpy)_2dppz]^{2+}$ tri-*n*-propylamine (TPrA) system, the detection limit calculation for this biosensor, and the reproducibility of this biosensor in batch and between batches (PDF).

AUTHOR INFORMATION

Corresponding Authors

*Tel.: +86-23-68252277. Fax: +86-23-68253172. E-mail: yqchai@swu.edu.cn.
*E-mail: yuanruo@swu.edu.cn.

ORCID

Ya-qin Chai: 0000-0003-4392-9592
Ruo Yuan: 0000-0003-3664-6236

DOI: 10.1021/acs.analchem.8b05001
Anal. Chem. 2019, 91, 3452−3458

Notes

The authors declare no competing financial interest.

■ ACKNOWLEDGMENTS

This work was financially supported by the National Natural Science Foundation of China (21775124, 21575116, and 21675129) and the Fundamental Research Funds for the Central Universities, China (XDJK2017A001).

■ REFERENCES

(1) Hu, L. Z.; Xu, G. B. *Chem. Soc. Rev.* **2010**, *39*, 3275−3304.
(2) Irkham; Watanabe, T.; Fiorani, A.; Valenti, G.; Paolucci, F.; Einaga, Y. *J. Am. Chem. Soc.* **2016**, *138*, 15636−15641.
(3) Li, M. X.; Feng, Q. M.; Zhou, Z.; Zhao, W.; Xu, J. J.; Chen, H. Y. *Anal. Chem.* **2018**, *90*, 1340−1347.
(4) Lv, Y. Q.; Chen, S. Y.; Shen, Y. F.; Ji, J. J.; Zhou, Q.; Liu, S. Q.; Zhang, Y. J. *J. Am. Chem. Soc.* **2018**, *140*, 2801−2804.
(5) Han, F. F.; Jiang, H.; Fang, D. J.; Jiang, D. C. *Anal. Chem.* **2014**, *86*, 6896−6902.
(6) Liu, X.; Jiang, H.; Fang, Y.; Zhao, W.; Wang, N. Y.; Zang, G. Z. *Anal. Chem.* **2015**, *87*, 9163−9169.
(7) Lu, J.; Getz, G.; Miska, E. A.; Alvarez-Saavedra, E.; Lamb, J.; Peck, D.; Sweet-Cordero, A.; Ebert, B. L.; Mak, R. H.; Ferrando, A. A.; Downing, J. R.; Jacks, T.; Horvitz, H. R.; Golub, T. R. *Nature* **2005**, *435*, 834−838.
(8) Croce, C. M.; Calin, G. A. *Cell* **2005**, *122*, 6−7.
(9) Zhang, P.; Lin, Z. F.; Zhuo, Y.; Yuan, R.; Chai, Y. Q. *Anal. Chem.* **2017**, *89*, 1338−1345.
(10) Peng, L. C.; Zhang, P.; Chai, Y. Q.; Yuan, R. *Anal. Chem.* **2017**, *89*, 5036−5042.
(11) Liang, W. B.; Fan, C. C.; Zhuo, Y.; Zheng, Y. N.; Xiong, C. Y.; Chai, Y. Q.; Yuan, R. *Anal. Chem.* **2016**, *88*, 4940−4948.
(12) Nie, Y. M.; Zhang, P.; Wang, H. J.; Zhuo, Y.; Chai, Y. Q.; Yuan, R. *Anal. Chem.* **2017**, *89*, 12821−12827.
(13) Han, K.; Lei, Q.; Jia, H. Z.; Wang, S. B.; Yin, W. N.; Chen, W. H.; Cheng, S. X.; Zhang, X. Z. *Adv. Funct. Mater.* **2015**, *25*, 1248−1257.
(14) Qi, H. L.; Li, M.; Dong, M. M.; Ruan, S. P.; Gao, Q.; Zhang, C. X. *Anal. Chem.* **2014**, *86*, 1372−1379.
(15) Tan, W. H.; Donovan, M. J.; Jiang, J. H. *Chem. Rev.* **2013**, *113*, 2842−2862.
(16) Jiang, Y.; Pan, X. S.; Chang, J.; Niu, W. J.; Hou, W. J.; Kuai, H. L.; Zhao, Z. L.; Liu, J.; Wang, M.; Tan, W. H. *J. Am. Chem. Soc.* **2018**, *140*, 6780−6784.
(17) Mayne, L.; Lin, C. Y.; Christie, S. D. R.; Siwy, Z. S.; Platt, M. *ACS Nano* **2018**, *12*, 4844−4852.
(18) Wang, D.; Chai, Y. Q.; Yuan, Y. L.; Yuan, R. *Anal. Chem.* **2017**, *89*, 8951−8956.
(19) Chen, H.; Crum, M.; Chavan, D.; Vu, B.; Kourentzi, K.; Willson, R. C. *ACS Appl. Mater. Interfaces* **2018**, *10*, 31845−31849.
(20) Yang, B.; Chen, B. B.; He, M.; Yin, X.; Xu, C.; Hu, B. *Anal. Chem.* **2018**, *90*, 2355−2361.
(21) Wang, S. Z.; Kuai, L.; Huang, Y. C.; Yu, X.; Liu, Y. D.; Li, W. Z.; Chen, L.; Geng, B. Y. *Chem. - Eur. J.* **2013**, *19*, 240−248.
(22) Barrow, S. J.; Funston, A. M.; Wei, X.; Mulvaney, P. *Nano Today* **2013**, *8*, 138−167.
(23) Hu, L. Z.; Bian, Z.; Li, H. J.; Han, S.; Yuan, Y. L.; Gao, L. X.; Xu, G. B. *Anal. Chem.* **2009**, *81*, 9807−9811.
(24) Zhang, P.; Jiang, J.; Yuan, R.; Zhuo, Y.; Chai, Y. Q. *J. Am. Chem. Soc.* **2018**, *140*, 9361−9364.
(25) Han, J. G.; Jiang, Y. D.; Zhang, C. H.; Yang, Y. M.; Pang, D.; Song, Y. N.; Zhang, G. Q. *Ann. Surg. Treat. Res.* **2017**, *92*, 55−66.
(26) Li, P.; Xu, T.; Zhou, X.; Liao, L. Y.; Pang, G. L.; Luo, W.; Han, L.; Zhang, J. K.; Luo, X. Y.; Xie, X. B.; Zhu, K. C. *Cancer Med.* **2017**, *6*, 662−672.
(27) Li, H.; Qiu, Z. W.; Li, F.; Wang, C. L. *Oncol. Lett.* **2017**, *14*, 5865−5870.
(28) Linn, S. C.; Honkoop, A. H.; Hoekman, K.; vanderValk, P.; Pinedo, H. M.; Giaccone, G. *Br. J. Cancer* **1996**, *74*, 63−68.
(29) Jiang, J. M.; Lee, E. J.; Gusev, Y.; Schmittgen, T. D. *Nucleic Acids Res.* **2005**, *33*, 5394−5403.
(30) Yu, S.; Wang, Y. Y.; Jiang, L. P.; Bi, S.; Zhu, J. J. *Anal. Chem.* **2018**, *90*, 4544−4551.
(31) Porowska, H.; Paszkiewicz-Gadek, A.; Wolczynski, S.; Gindzienski, A. *Neoplasia* **2002**, *49*, 104−109.

DOI: 10.1021/acs.analchem.8b05001
Anal. Chem. 2019, 91, 3452−3458